Journal of
Synchrotron
Radiation

ISSN 0909-0495

Received 8 February 2007
Accepted 29 March 2007

Rapid characterization of molecular chemistry, nutrient make-up and microlocation of internal seed tissue

Peiqiang Yu,* H. Block, Z. Niu and K. Doiron

College of Agriculture and Bioresources, University of Saskatchewan, 51 Campus Drive, Saskatoon, Canada S7N 5A8. E-mail: peiqiang.yu@usask.ca

Wheat differs from corn in biodegradation kinetics and fermentation characteristics. Wheat exhibits a relatively high rate (23% h^{-1}) and extent (78% DM) of biodegradation, which can lead to metabolic problems such as acidosis and bloat in ruminants. The objective of this study was to rapidly characterize the molecular chemistry of the internal structure of wheat (cv. AC Barrie) and reveal both its structural chemical make-up and nutrient component matrix by analyzing the intensity and spatial distribution of molecular functional groups within the intact seed using advanced synchrotron-powered Fourier transform infrared (FTIR) microspectroscopy. The experiment was performed at the U2B station of the National Synchrotron Light Source at Brookhaven National Laboratory, New York, USA. The wheat tissue was imaged systematically from the pericarp, seed coat, aleurone layer and endosperm under the peaks at ~1732 (carbonyl C=O ester), 1515 (aromatic compound of lignin), 1650 (amide I), 1025 (non-structural CHO), 1550 (amide II), 1246 (cellulosic material), 1160, 1150, 1080, 930, 860 (all CHO), 3350 (OH and NH stretching), 2928 (CH_2 stretching band) and 2885 cm^{-1} (CH_3 stretching band). Hierarchical cluster analysis and principal component analysis were applied to analyze the molecular FTIR spectra obtained from the different inherent structures within the intact wheat tissues. The results showed that, with synchrotron-powered FTIR microspectroscopy, images of the molecular chemistry of wheat could be generated at an ultra-spatial resolution. The features of aromatic lignin, structural and non-structural carbohydrates, as well as nutrient make-up and interactions in the seeds, could be revealed. Both principal component analysis and hierarchical cluster analysis methods are conclusive in showing that they can discriminate and classify the different inherent structures within the seed tissue. The wheat exhibited distinguishable differences in the structural and nutrient make-up among the pericarp, seed coat, aleurone layer and endosperm. Such information on the molecular chemistry can be used for grain-breeding programs for selecting a superior variety of wheat targeted for food and feed purposes and for predicting wheat quality and nutritive value in humans and animals. Thus advanced synchrotron-powered FTIR technology can provide a greater understanding of the plant–animal interface.

Keywords: FTIR spectroscopic characteristics; wheat; molecular chemistry; nutrient make-up; cluster analysis.

1. Introduction

Wheat differs from corn in biodegradation kinetics and fermentation characteristics. Wheat exhibits a relatively higher rate (23% h^{-1} *versus* 10% h^{-1} for corn) and extent (72% DM *versus* 57% DM for corn) of rumen degradation. In ruminants, these fast degradation characteristics can lead to metabolic problems such as acidosis and bloat. The selection of wheat varieties has been one of several approaches undertaken to improve the nutritive value and nutrient utilization for both humans and animals.

The biological differences between cereal grains are related to molecular structural differences between the seeds. Most studies focus on total (or overall) chemical composition of seeds such as total protein and carbohydrates (structural and non-structural) using traditional 'wet' chemical analysis, which

has the big disadvantage of relying heavily on the use of harsh chemicals and derivatives, thereby altering the native structures and possibly generating artifacts (Budevska, 2002). The wet chemical analysis looks for a specific component through homogenization of the tissue and separation of the component of interest from the complex matrix that makes up the seed. As a result, information on the spatial origin and distribution of the component of interest is lost and the object of the analysis is destroyed (Budevska, 2002).

Synchrotron-powered Fourier transform infrared (FTIR) microspectroscopy can be used to identify molecular constituents in biological samples from their vibrational spectra in the mid-IR region, and is capable of exploring the molecular chemistry (structural make-up) within microstructures of biological tissues at a cellular level without destruction of internal structures at highly spatial resolutions (3–10 μm) (Wetzel *et al.*, 1998; Miller, 2000, 2002; Marinkovic *et al.*, 2002; Pietrzak & Miller, 2005; Miller & Dumas, 2006; Marinkovic & Chance, 2006). The chemical information (qualitative and quantitative analytical results) can be linked to structural information (Budevska, 2002).

The objective of this study was to rapidly characterize and image the molecular chemistry of the inherent structures of wheat to reveal structural chemical features and nutrient component matrix in the seed tissue by using rapid direct non-destructive synchrotron-powered FTIR microspectroscopy.

2. Materials and methods

2.1. Synchrotron FTIR window preparation and wheat seed tissue

Wheat seed (cv. AC Barrie) was obtained from Pierre Hucl, Crop Development Center, The University of Saskatchewan, Canada. Detailed studies of the wheat seed in terms of chemical composition, *in situ* degradation kinetics, energy values and predicted nutrient supply have been conducted in our laboratory. The wheat seeds were cut into thin cross sections (6 μm thick) using a microtome at The Western College of Veterinary Medicine, University of Saskatchewan. Unstained cross sections were transferred to BaF_2 windows (size: 13 mm × 1 mm disc; Spectral Systems, NY, USA) for synchrotron FTIR microspectroscopic analysis in transmission mode.

2.2. Photomicrographs of the cross sections of wheat seed tissues

Photomicrographs of the cross section of the wheat tissue were recorded using a microscope linked to a digital camera from the FTIR BaF_2 window.

2.3. Synchrotron light source and synchrotron FTIR microspectroscopy

The experiment was carried out on beamline U2B, The Center for Synchrotron Biosciences (Case Western Reserve University) at the National Synchrotron Light Source located in Brookhaven National Laboratory, New York, USA. The beamline is equipped with a FTIR spectrometer (Nicolet Magna 860) with KBr beamsplitter and a mercury cadmium telluride (MCT-A) detector coupled to an IR microscope (Nic Plan, Nicolet Instruments, Madison, WI, USA). The bench was configured to use collimated synchrotron light (beam energy 800 MeV) through an external input on the spectrometer. The modulated light was passed through the Nic Plan IR microscope to perform transmission microscopy.

The IR spectra were collected in the mid-IR range, 4000–800 cm^{-1}, at a resolution of 4 cm^{-1} with 64 scans co-added and an aperture setting of ∼10 μm × 10 μm. This aperture size was chosen because (i) the size was within the cellular dimension and (ii) it was the best for obtaining a good signal-to-noise ratio for spectral mapping of the wheat tissue. To minimize IR absorption by CO_2 and water vapor in the ambient air, the optics were purged using dry N_2. A background spectrum was collected from an area free of sample. Mapping steps were equal to the aperture size. Stage control, data collection and processing were performed using *OMNIC* 7.2 software (Thermo-Nicolet, Madison, WI, USA). Scanned visible images were obtained using a charge-coupled-device (CCD) camera linked to the IR images (objective ×32). The total time for the mapping was 4 h 38 min.

Spatial information was obtained by microspectroscopic area mapping, where the tissue on the microscope stage was translated along the *x* and *y* axes, thus positioning different parts of the designated tissues in the synchrotron IR beam. The motorized computer-controlled stage was programmed to trace the designated areas of the tissues. After measuring the spectra of all regions of interest, spectral information was related to the respective visible images. As a result, spectral data sets were formed with the *xy* plane, corresponding to the scanned area of the sample, while the *z* plane contained the spectral information. Chemical functional group images (such as amide I, aromatic compounds, carbonyl ester) were generated by plotting the intensity of synchrotron IR absorption bands as a function of their *xy* position (Budevska, 2002). Different coverage of the sample could also be achieved by varying the step size and the dimensions of the image mask (aperture size). The big advantage of using a synchrotron beam with FTIR spectroscopy to map the tissues is that spatial resolution to diffraction limits is achievable (Wetzel *et al.*, 1998; Miller, 2002).

2.4. Spectral data analysis and imaging molecular chemistry

The spectral data of the tissues were collected and analyzed after the correction of the background spectrum using *OMNIC* 7.2 software. A baseline correction was applied to generate the final spectra. The data can be displayed either as a series of spectroscopic images collected at individual wavelength or as a collection of IR spectra obtained at each pixel position in the image.

Molecular chemistry of functional groups from the pericarp, seed coat, aleurone layer to endosperm was imaged under peaks at ∼1732, 1515, 1650, 1550, 1025, 1246, 1160, 1150, 1080, 929, 860, 3350, 2928 and 2885 cm^{-1} using the *OMNIC* 7.2

software (Wetzel *et al.*, 1998; Himmelsbach *et al.*, 1998; Wetzel, 2001). Peak ratio images of molecular functional groups, representing the distribution of the biological component ratio (also called nutrient component ratio) of the tissue, were obtained by dividing the area under one molecular functional group band (*e.g.* amide I, $\sim$1650 cm^{-1}) by the area under another molecular functional group band (*e.g.* non-structural CHO, 1025 cm^{-1}) at each pixel (pixel size 10 µm $\times$ 10 µm). False-color maps derived from the area under particular spectral features were used to represent distribution and intensity of functional groups across the area of interest.

2.5. Multivariable statistical analysis for synchrotron-based FTIR spectra

Multivariate analyses, *i.e.* hierarchical cluster analysis and principal component analysis, were performed using *Statistica* 6.0 software (StatSoft, Tulsa, OK, USA) to classify the inherent structures of the wheat tissue.

3. Results and discussion

3.1. Visible image fails to reveal molecular structural–chemical feature

The nutritive value or nutrient availability of wheat in both humans and animals is highly related to its inherent structure and the molecular chemical make-up. Fig. 1 illustrates the intrinsic structure of the wheat tissue (6 µm-thick cross section) from the pericarp on the outside of the seed, to the seed coat, through to the aleurone layer and part of the endosperm. Usually the pericarp forms a tough outer covering on the seed kernel providing protection for the interior components. The seed coat is found between the pericarp and the aleurone layer. Aleurone cells play an important role during seedling development. The endosperm consists of cells filled mainly with starch granules. The photomicrograph of the tissue, however, is not informative with respect to molecular chemical features (or chemical make-up) of the inherent structures at a sub-cellular spatial resolution.

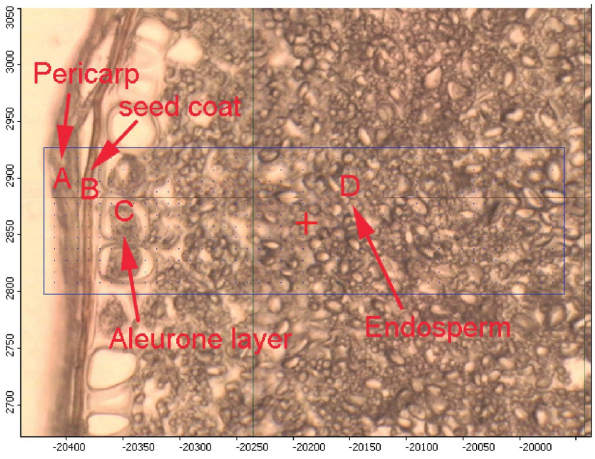

Figure 1
Photomicrograph of the cross section of wheat tissue (6 µm) showing the intrinsic structure of wheat from pericarp (outside of seed) (A), seed coat (B), aleurone layer (C) and endosperm (D).

3.2. Imaging molecular chemistry to reveal internal structural features

Mid-IR spectroscopy (4000–600 cm^{-1}) measures the contribution of particular organic and inorganic functional groups within molecules from their induced vibrations (Marinkovic *et al.*, 2002; Wetzel, 2001). A drawback of globar-sourced FTIR microspectroscopy is the diffraction effects which are a result of the aperture being decreased to limit the field of view to a small region of interest. At the same time, less light overall results in a decrease in the signal-to-noise ratio. For this kind of study on a plant tissue's molecular structural–chemical features for which spectral data need to be collected at the diffraction limit (a few micrometers) in each spatial dimension, only advanced synchrotrons and free-electron lasers can be used to achieve this. Furthermore, the brightness of conventional bench-top IR sources is lower by two to three orders of magnitude (Raab & Martin, 2001). Based on the advantages offered by synchrotron FTIR microspectroscopy, the molecular chemistry of wheat was imaged, enabling the detection of molecular chemical features of biological samples at high spatial resolutions without destructing the inherent structure of the tissue (Miller & Dumas, 2006; Marinkovic & Chance, 2006).

Fig. 2 shows color maps of functional groups from a cross section of the wheat tissue and single-pixel spectra from a 10 µm $\times$ 10 µm sample area.[1] It shows visible and chemical images in false-color representation of the chemical component intensities, and spectra at various pixels. Using synchrotron FTIR microspectroscopy, the distribution and relative concentration of the chemical functional groups associated with the wheat tissue inherent structures were mapped. The IR images were taken from the region of the visible image outlined by the rectangle area. The molecular chemistry of functional groups from the pericarp, seed coat, aleurone layer and part of endosperm was imaged under peaks at 1732 (stretching vibration of carbonyl C$=$O), 1515 (aromatic character of lignin; semicircle ring stretch), 1025 (non-structural CHO), 1650 (amide I C$=$O), 1550 (amide II N$-$H and C$-$N), 1246 (cellulosic), 1160, 1150, 1080, 930, 860 (all CHO), 3350 (NH and OH stretching), 2928 (CH_2 stretching vibrations) and 2885 cm^{-1} (CH_3 stretching vibrations). The molecular functional group band assignments (for cereal grain) were applied according to the published literature (Himmelsbach *et al.*, 1998; Wetzel *et al.*, 1998, 2003).

3.2.1. Imaging lipid (carbonyl C$=$O) and methylesterified pectins within the intact wheat tissue. The dominant absorption features of the lipid spectrum are found in the region 2800–3000 cm^{-1}, and were assigned by analogy with the IR spectra of alkanes. They are predominantly asymmetric and symmetric stretching vibrations of the CH_3 ($\sim$2956 and 2874 cm^{-1}) and CH_2 ($\sim$2922 and 2852 cm^{-1}) groups of the acyl chains (Miller, 2000; Jackson & Mantsch, 2000; Wetzel & LeVine, 2000). Wetzel & LeVine (2000) reported that the

[1] Further examples are available as supplementary data from the IUCr electronic archives (Reference: YS5001). Services for accessing these data are described at the back of the journal.

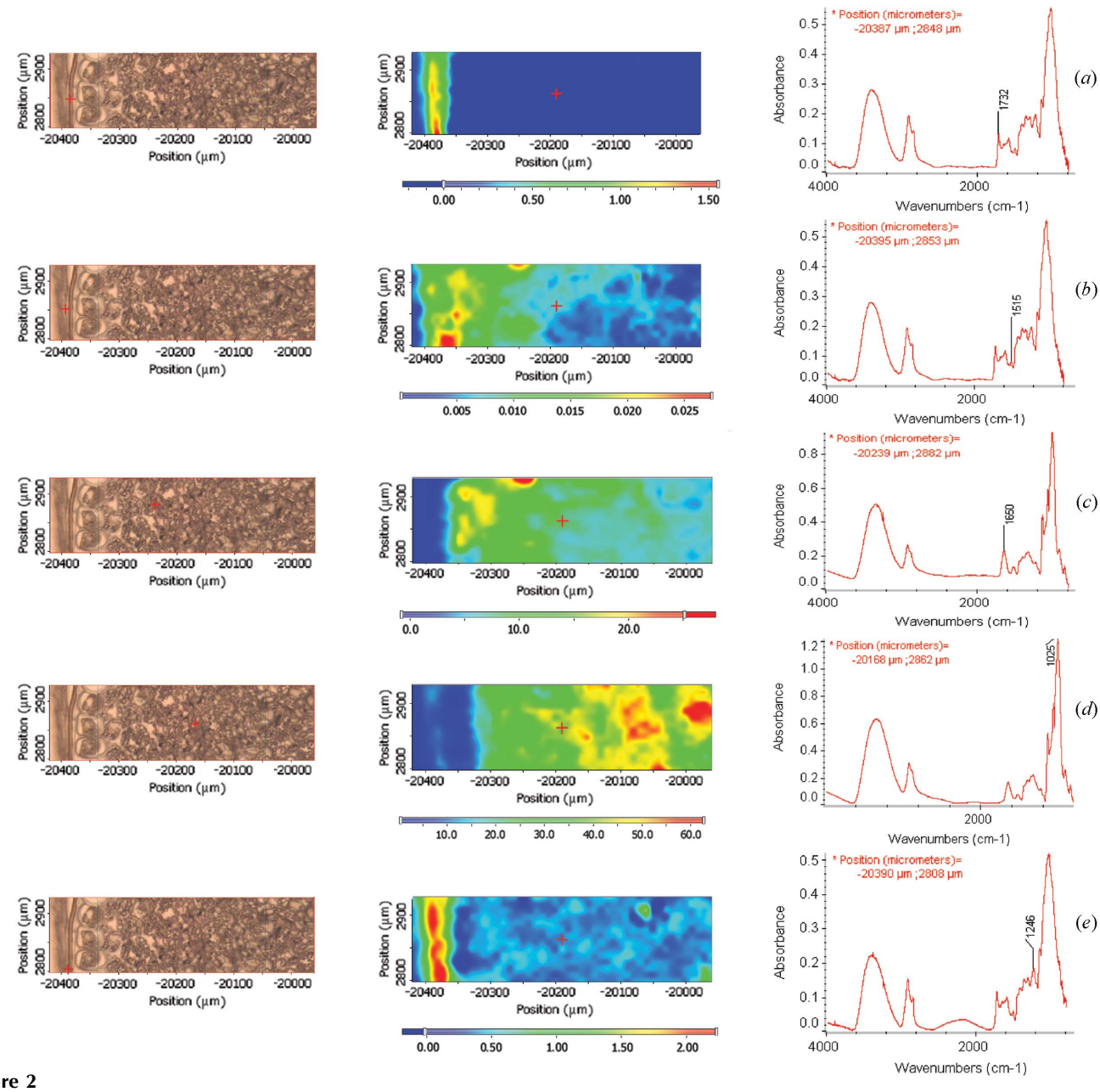

Figure 2
Molecular functional group images of the wheat seed tissue from the pericarp (outside), seed coat, aleurone layer and endosperm. From left to right: visible image; chemical image; spectra corresponding to the pixel at the cross-hair in the visible image (spectrum pixel size 10 μm × 10 μm). Area under (*a*) 1732 cm^{-1} peak (carbonyl C═O); (*b*) 1515 cm^{-1} peak (aromatic compound); (*c*) 1650 cm^{-1} peak (amide I); (*d*) 1025 cm^{-1} peak (starch); (*e*) 1246 cm^{-1} peak (cellulosic materials).

long-chain CH_2 functional group is represented at ∼2927 cm^{-1} (asymmetric stretch) and ∼1469 cm^{-1} (CH bend). The small band at ∼3015 cm^{-1} indicates the presence of unsaturation (CH attached to C═C). As expected from the greater number of CH_2 groups, the corresponding peak intensities are 10–20 times greater than those of CH_3. The frequency of the CH_2 stretching absorptions provides a useful probe of the lipid bilayer order, lower frequencies being associated with a higher degree of conformational order (Jackson & Mantsch, 2000). In addition, the strong band at ∼1732 cm^{-1} arises from a stretching vibration of the carbonyl ester C═O groups in the lipid (Marinkovic *et al.*, 2002; Wetzel *et al.*, 1998; Miller, 2000). All these bands have been used to indicate lipid characteristics. The characteristics of lipid chain length, branching and unsaturation are usually inferred by comparing contributions of carbonyl ester C═O, CH_3, CH_2 and CH—C═C absorptions (Wetzel & LeVine, 2000).

Fig. 2(*a*) shows the chemical image under area at ∼1732 cm^{-1} (mapping baseline: 1751–1714 cm^{-1}) showing the distribution of lipids. The band at ∼1732 cm^{-1} is due to the carbonyl group (C═O) stretching vibration in the ester linkage in the pericarp and seed coat. The seed coat contained the highest intensity of the carbonyl C═O molecules. The aleurone layer and endosperm areas contain little lipid. The

spectra on the right in each figure correspond to the pixel in the cross-hair and were selected to represent the value of the integrated peak. The represented spectra show a wide variety of spectral characteristics which manifest the chemical composition in different morphological parts of the seed. In plant leaves the $\sim$1732 cm^{-1} feature may also arise from methylesterified pectins (Vogel *et al.*, 2002), not only lipid in cereal grain (Wetzel *et al.*, 1998).

3.2.2. Imaging aromatic compounds (lignin) within the intact tissue. The unique absorption band of lignin is found at $\sim$1515 cm^{-1} in the mid-IR region of the electromagnetic spectrum. This is considered to be indicative of the aromatic character of the lignin. An aromatic compound gives two major bands at $\sim$1600 and 1515 cm^{-1}, resulting from quadrant and semicircle ring stretching, respectively (Colthup *et al.*, 1990). These are well exemplified in the lignin spectrum which shows bands at $\sim$1600 and $\sim$1515 cm^{-1}. The first of these bands has possible interference with other bands. The second of these bands, with its peak at $\sim$1515 cm^{-1}, shows no significant interference with any other bands and is thus an excellent diagnostic criterion for identifying aromatics. Fig. 2(*b*) is a chemical image under the area at $\sim$1515 cm^{-1} (mapping baseline: 1529–1487 cm^{-1}), showing the spatial lignin distribution and concentration of the area under peaks centered at 1515 cm^{-1}. The IR image data were recorded in the area outlined by the rectangle of the visible image. The 1515 cm^{-1} band (Wetzel *et al.*, 1998; Himmelsbach *et al.*, 1998; Colthup *et al.*, 1990) corresponds to the stretch associated with para-substituted benzene rings and can be associated with aromatic species present in the pericarp, seed coat and aleurone layer of the wheat tissue.

3.2.3. Imaging amide I and II (protein) within the intact tissue. The protein spectrum has two primary features, the amide I ($\sim$1650 cm^{-1}) and amide II ($\sim$1550 cm^{-1}) bands, which arise from specific stretching and bending vibrations of the protein backbone. The amide I band arises predominantly from the C═O stretching vibration (80%) of the amide C═O group plus C—N stretching vibration (20%) (Jackson & Mantsch, 2000). The vibrational frequency of the amide I band is particularly sensitive to protein secondary structure (Kemp, 1991; Miller, 2002; Martin, 2002; Wetzel *et al.*, 2003; Marinkovic *et al.*, 2002; Marinkovic & Chance, 2006) and can be used to predict protein secondary structures (Yu, 2005, 2006). The amide II band [predominantly from N—H bending vibration (60%) coupled to C—N stretching (40%)] is also used to assess protein conformation (Jackson & Mantsch, 2000). However, as it arises from complex vibrations involving multiple functional groups, it is less useful for protein structure prediction than the amide I band (Jackson & Mantsch, 2000). Fig. 2(*c*) is a chemical image of the area under $\sim$1650 cm^{-1} (mapping baseline: $\sim$1714–1579 cm^{-1}) and 1550 cm^{-1} (mapping baseline: $\sim$1576–1487 cm^{-1}), showing the area under the $\sim$1650 cm^{-1} and 1550 cm^{-1} peak attributed to protein absorption (amide I and II, respectively). The amide I (1650 cm^{-1}) and amide II (1550 cm^{-1}) bands are characteristics of C═O, C—N and N—H bonds in the protein backbone and are indicators of the area of the sample where protein is present. Fig. 2(*c*) shows that the pericarp and seed coat region has no protein associated with it and that protein concentration is highest in the aleurone layer. The endosperm areas also contain amide I and II bands.

3.2.4. Imaging structural and non-structural CHO within the intact tissue. The major absorption bands from carbohydrates are found in the $\sim$1180–950 cm^{-1} region of the spectrum (Mathlouthi & Koenig, 1986) and are attributed to C–O stretching vibrations. The bands in this region are very complicated. When studying cereal grain materials, it is customary to look for structural carbohydrates such as cellulose or hemicellulose (Wetzel *et al.*, 1998; Wetzel, 2001) and non-structural carbohydrates such as starch (Wetzel *et al.*, 1998). A peak area at the $\sim$1420 cm^{-1} band can be used to look for irregular depositions of a particular type of carbohydrate called β-glucan (Wetzel *et al.*, 1998). In the portion of the spectrum from 1550 to 800 cm^{-1}, strong carbohydrate bands are present for both structural and non-structural carbohydrate, particularly in the 1100–1025 cm^{-1} region. A major difference between these two forms of carbohydrate is the presence of bands of moderate intensity at approximately 1420, 1370 and 1335 cm^{-1} which indicate characteristics of structural carbohydrates (Wetzel *et al.*, 1998; Wetzel, 2001). Carbohydrate band peaks between 1100 and 1025 cm^{-1} depend on whether the carbohydrate is structural or non-structural. A peak at $\sim$1025 cm^{-1} is indicative of non-structural carbohydrate such as starch in endosperm of cereal grain (Wetzel *et al.*, 1998; Wetzel, 2001). Starch is a branched α-(1,4)-glucose polymer and is one of the principal energy storage forms for plants. A peak at $\sim$1246 cm^{-1} is used to indicate a structural carbohydrate such as cellulosic material (Wetzel *et al.*, 1998). Cellulose is a β-(1,4)-glucose polymer, laid down in long parallel strands. Fig. 2(*d*) is the chemical image under area at $\sim$1025 cm^{-1} (mapping baseline: $\sim$1068–957 cm^{-1}), showing that the pericarp, seed coat and aleurone regions have no non-structural CHO (starch), while the endosperm region contains a high amount of non-structural CHO. Fig. 2(*e*) is the chemical image under area at $\sim$1246 cm^{-1} (mapping baseline: $\sim$1288–1214 cm^{-1}), revealing the ultra-spatial distribution of cellulosic material and its concentration. It shows that the pericarp and seed coat contain high amounts of cellulosic materials, but the aleurone layer and endosperm region contain little structural CHO. [Figs. 2(*f*)–2(*m*) (see Supplementary material) show the spatial distribution of various carbohydrate bands. The spectrum for carbohydrates assignments are very complicated and are not fully understood in a complex plant system.]

3.2.5. Imaging molecular functional groups ratios within the intact tissue. Using molecular functional group ratios has a big advantage because the ratios indicate relative biological component (also called nutrient component) content, and can be used to determine food or feed quality and nutritive values in both humans and animals. Fig. 3 illustrates a molecular functional group ratio image, showing the peak area ratio of protein amide I and total carbohydrate and represents the distribution and intensity of the area under the $\sim$1650 cm^{-1} band divided by the area under the peaks between 1180 and

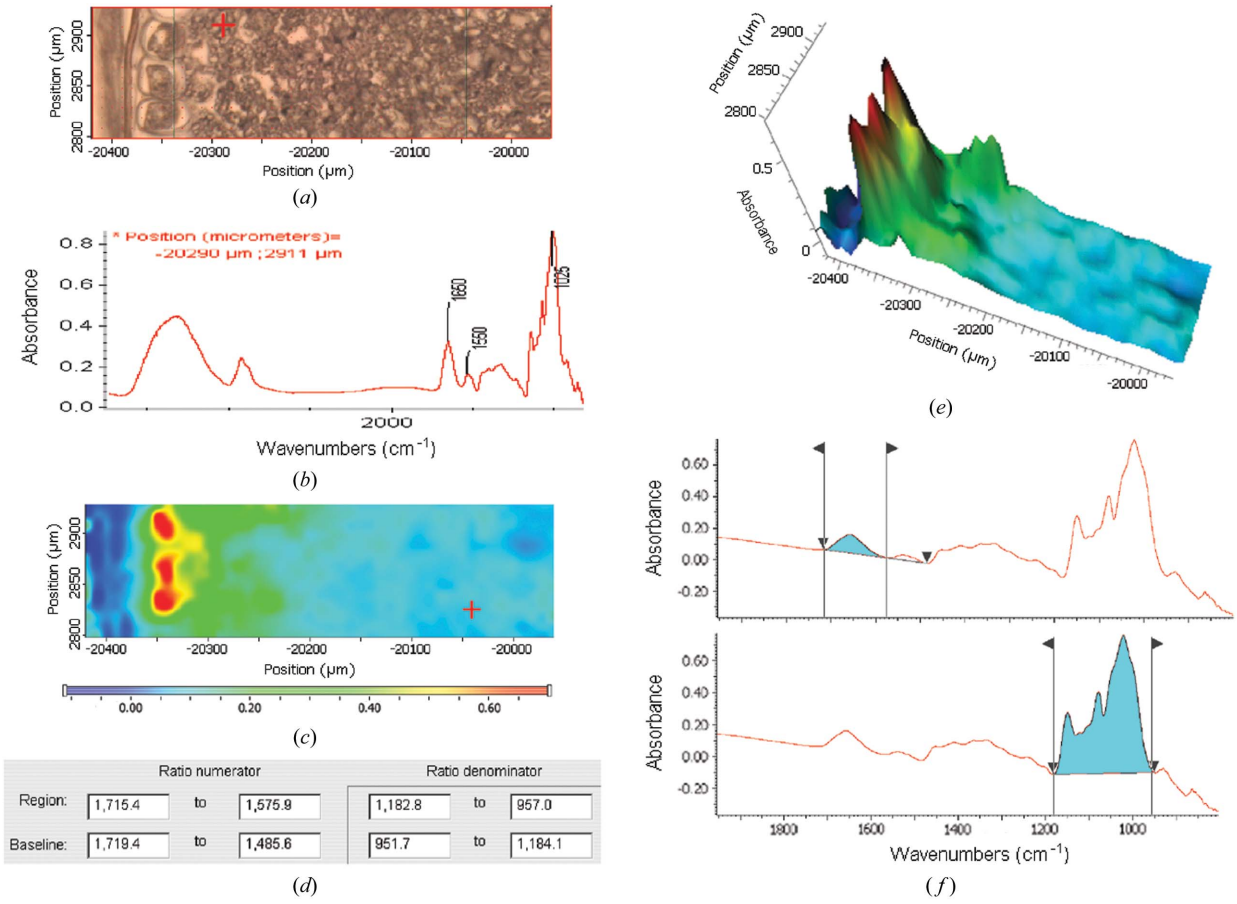

Figure 3
Molecular functional group peak area ratio: area under the protein amide I (1650 cm^{-1}) bands divided by the area under the peaks between ~1180 and 950 cm^{-1} at each pixel (pixel size 10 μm ×10 μm) representing protein-to-total-carbohydrate ratio in the wheat seed tissue. (*a*) Visible image. (*b*) Spectra corresponding to the pixel at the cross-hair in the visible image. (*c*) Chemical ratio image: protein to carbohydrate ratio. (*d*) Region and baseline of protein amide I and II and carbohydrate. (*e*) Three-dimensional image. (*f*) Ratio image profile set-up.

950 cm^{-1} at each pixel. The results show that the highest ratio of protein amide I to carbohydrate is in the aleurone layer. Fig. 3 clearly shows three high peaks from three aleurone cells in the tissue.

The above work clearly shows that imaging molecular chemistry across plant seed tissues at ultra-spatial resolution could be accomplished using FTIR microspectroscopy powered by bright synchrotron light. Such information can be analyzed for crucial clues of the intrinsic seed structures in relation to biodegradation characteristics in both humans and animals.

3.3. Similar morphological parts exhibit similar spectral characteristics

Fig. 4 presents molecular spectra[2] from the pericarp, aleurone layer and endosperm, showing that similar morphological parts of the seed exhibit similar spectral characteristics, which indicates similar molecular functional groups and thus similar biological (or nutrient) components. All pixels in the pericarp show spectral peaks at ~1732, 1600, 1510, 1420, 1375, 1320, 1246, 1160 and 1035 cm^{-1}. All pixels in the aleurone layer show spectral peaks at ~1732, 1650, 1550, 1510, 1460, 1380, 1320, 1246, 1160 and 1055 cm^{-1}. All pixels in the endosperm region show spectral peaks at 1650, 1550, 1450, 1150, 1080 and 1025 cm^{-1}. This indicates that pericarp contains a higher concentration of lignin (1510 cm^{-1}), cellulose (1246 cm^{-1}) and lipid (1732 cm^{-1}) materials and little concentration of protein (1650 cm^{-1} for the amide I band and 1550 cm^{-1} for the amide II band). Contrary to that, the aleurone layer has practically no lignin (1510 cm^{-1}) and higher protein (1650 and 1550 cm^{-1}), and the endosperm region has higher starch (1025 cm^{-1}).

3.4. Discriminating and classifying molecular chemical make-up of the internal structures

3.4.1. Using agglomerative hierarchical cluster analysis. The function of cluster analysis (CLA) is to perform a (agglomerative hierarchical) cluster analysis of an IR spectra data set and display the results as dendrograms. First, it calculates a distance matrix, containing information on the similarity of the spectra. Then, in hierarchical clustering, the

[2] Further examples are available as supplementary data from the IUCr electronic archives (Reference: YS5001). Services for accessing these data are described at the back of the journal.

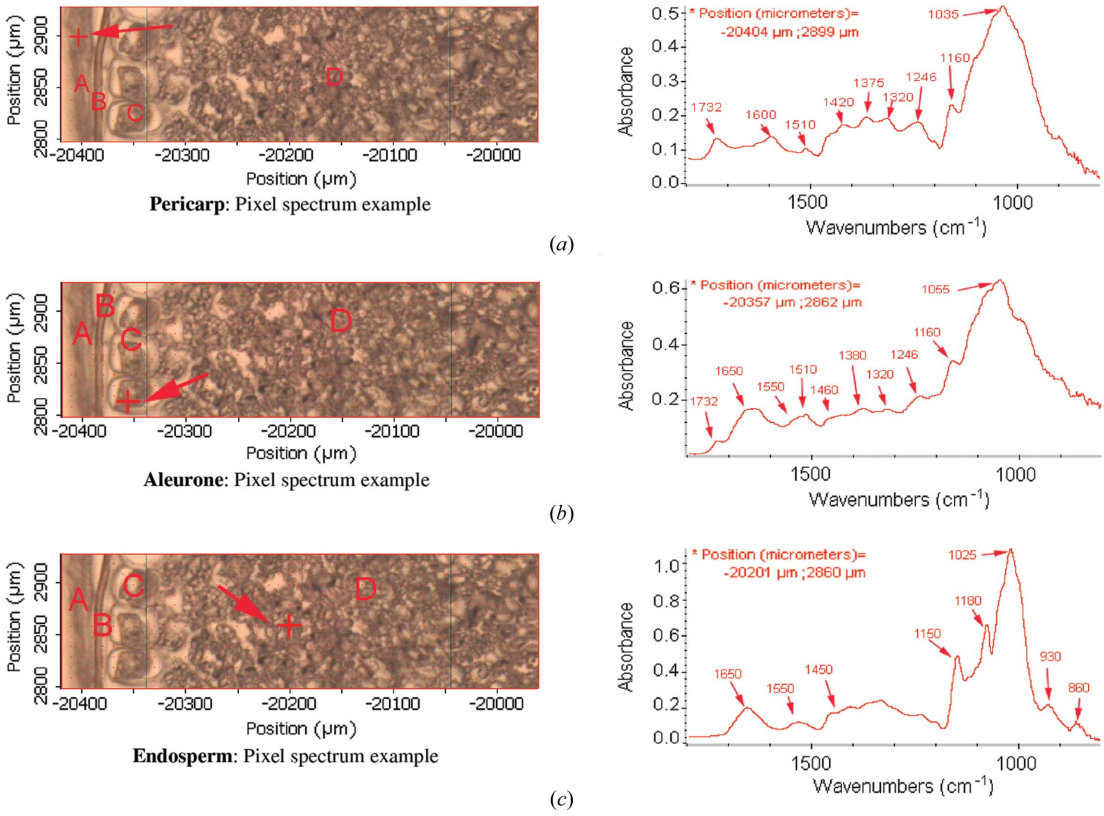

Figure 4
Ultra-spatial synchrotron-based spectra of (*a*) the pericarp, (*b*) the aleurone layer, (*c*) the endosperm of wheat tissues selected from corresponding areas of the visible images, showing that similar morphological parts exhibit similar spectral characteristics and chemical composition (A = pericarp; B = seed coat; C = aleurone layer; D = endosperm).

algorithm searches within the distance matrix for the two most similar IR spectra (minimal distance). These spectra are combined into a new object (called a 'cluster' or 'hierarchical group'). The spectral distances between all remaining spectra and the new cluster are re-calculated (Cytospec, 2004). It is a technique which clusters IR spectra based on similarity with other spectra. In this study, the Ward's algorithm was used without any prior parameterization of the spectral data (used original spectral data in fingerprint region ~1800–800 cm^{-1}). This method highlights the ability to distinguish the difference in the inherent structures and molecular chemical make-up between different morphological layers within the tissue. Fig. 5 shows the CLA clusters within the intact wheat tissue to compare the molecule spectra from the endosperm (containing easily digested compounds: non-structural CHO and protein) with the spectra from the pericarp region

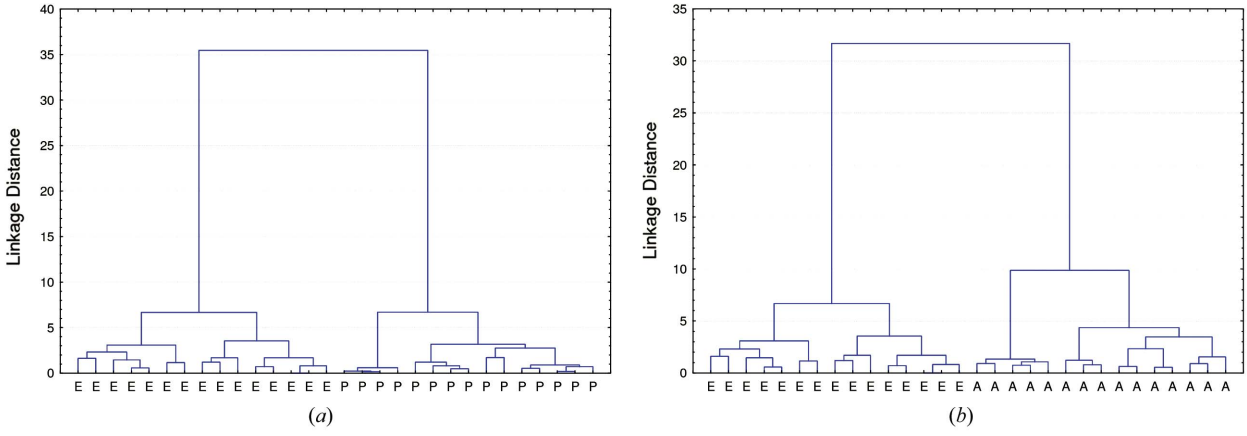

Figure 5
CLA clusters of wheat (cv. AC Barrie) inherent structures, showing that the clusters in the pericarp, aleurone layer and endosperm are different [CLA analysis: (i) fingerprint spectral region: 1800–800 cm^{-1}; (ii) distance method: Euclidean; (iii) cluster method: Ward's algorithm]. (*a*) Compared molecular spectral characteristics of pericarp (P) *versus* endosperm (E). (*b*) Compared molecular spectral characteristics of the aleurone layer (A) *versus* endosperm (E).

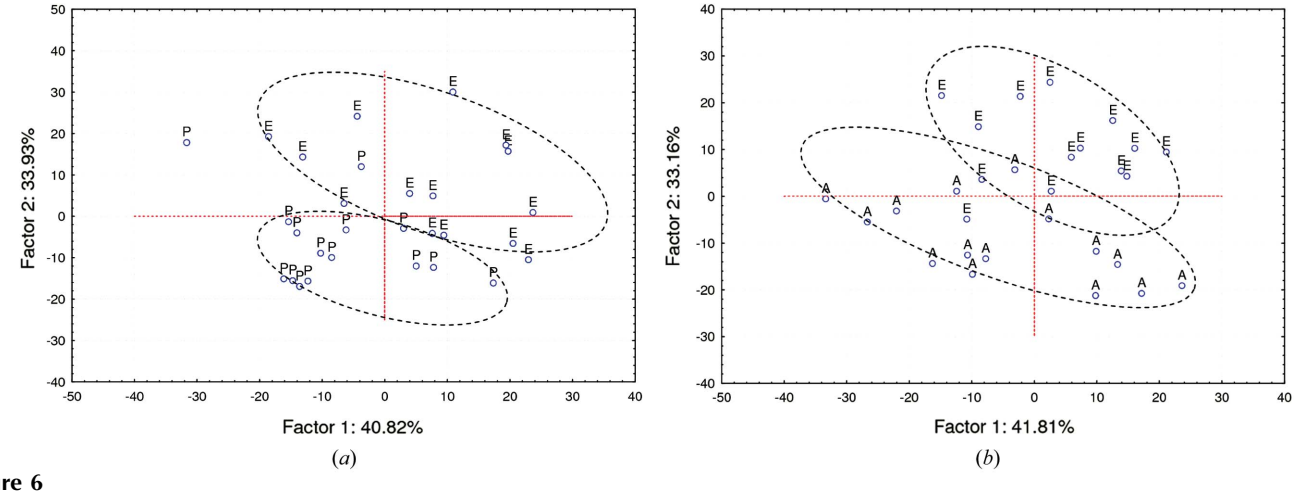

Figure 6
PCA analysis of synchrotron-based FTIR wheat molecular spectrum in fingerprint region 1800–800 cm^{-1} obtained from the pericarp (P), aleurone layer (A) and endosperms (E): scatter plots of the first principal components (PC1) *versus* the second principal components (PC2). (*a*) Compared molecular spectral characteristics of pericarp (P) *versus* endosperm (E). (*b*) Compared molecular spectral characteristics of the aleurone layer (A) *versus* endosperm (E).

(containing digestion-resistant compounds: aromatic lignin and cellulosic compounds) (Fig. 5*a*) and aleurone layer (containing easily digested compound: protein) (Fig. 5*b*). The results clearly show that the clusters are different between different structures (pericarp and aleurone *versus* endosperm) within intact tissue. No published results have been found for comparison.

3.4.2. Using principal component analysis. Principal component analysis (PCA) is a statistical data-reduction method. It transforms the original set of variables into a new set of uncorrelated variables called principal components (PCs). The first few PCs will typically account for >95% variance. The purpose of PCA is to derive a small number of independent linear combinations (PCs) from a set of variables that retain as much of the information in the original variables as possible. This analysis allows the relationships between p quantitative characters (*e.g.* molecular functional groups, aromatic lignin and cellulosic compounds) observed on n samples (*e.g.* FTIR molecular spectra) to be studied globally. The basic idea is to extract, in a multiple variable system, one, two or sometimes more PCs that carry maximum information. These components are independent (orthogonal) of each other and the first factor generally represents maximum variance. As factors are extracted, they account for less and less variability and the decision of when to stop basically depends on the point when there is only very little significant variability left, or merely random noise. Thus, the reduction of data provides a new coordinate system where axes (eigenvectors) represent the characteristic structural information of the data and the spectra may then be simply described as a function of specific properties, and no longer as a function of intensities. The outcome of such an analysis can be presented either as two-dimensional (two PCs) or three-dimensional (three PCs) scatter plots (Sockalingum *et al.*, 1998). In this molecular chemistry study, the PCA was used to identify the main sources of variation in the synchrotron-based FTIR molecular spectra in the fingerprint region ~1800–800 cm^{-1} of the intact tissue within cellular dimensions and identify the structural make-up features that differ between different structural regions (or different morphological parts) within the intact tissue. Fig. 6 show results from PCA analysis of the molecular spectrum data obtained from the pericarp, aleurone layer and endosperm. The first two PCs (obtained after data reduction) were plotted and show that the two inherent structures [pericarp *versus* endosperm in Fig. 6(*a*) and pericarp *versus* endosperm in Fig. 6(*b*)] can be grouped in separate ellipses. The first three PCs explain 40.8, 33.9 and 13.9%, and 41.8, 33.2 and 15.5% of the variation in the structural molecular spectrum data set between the pericarp and endosperm, and aleurone and endosperm, respectively. Therefore PCA distinguished the difference between the different structures. These results indicate that the structural chemical make-up between the structures is fully distinguished. No publications have been found using PCA analysis for feed quality research, so no comparison could be made.

4. Conclusions

In conclusion, with synchrotron-powered FTIR microspectroscopy, ultra-spatial images of molecular chemistry from intact seed tissues could be generated. This molecular chemical information can be linked to structural and nutritional information. Both CLA and PCA methods gave satisfactory analytical results and are conclusive in showing that they can discriminate and classify different inherent structures within the intact seed tissue. The wheat exhibited distinguished differences in the structural and nutrient make-up among the pericarp, seed coat, aleurone layer and endosperm. Such information on the microstructural chemical features of wheat can also be used for grain breeding programs for selecting a superior variety of wheat for targeted food and feed purposes and for prediction of wheat quality and nutritive value in humans and animals. The advanced synchrotron-

based FTIR microspectroscopy technology provides a greater understanding of the plant–animal interface.

This research has been supported by grants from the Natural Sciences and Engineering Research Council of Canada (NSERC, Individual Discovery Grant) and Saskatchewan Agricultural Development Fund (ADF). The National Synchrotron Light Source in Brookhaven National Laboratory (NSLS-BNL, New York, USA) is supported by US Department of Energy contract DE-AC02-98CH10886. The Center for Synchrotron Biosciences, The Center for Proteomics at Case Western Reserve University is supported by the National Institute for Biomedical Imaging and Bioengineering under contract P41-EB-01979. We are grateful to Pierre Hucl (University of Saskatchewan) for providing the AC Barrie wheat sample; John McKinnon, Colleen Christensen and David Christensen (University of Saskatchewan) for support; Jennifer Bohon, Nebojsa Marinkovic, Lisa Miller, Wang Qi, Alexander Ignatov (NSLS-BNL, New York, USA) and Kevin Doiron and Hushton Block (University of Saskatchewan) for helpful data collection at U2B and U10B experimental stations; and Tim May for helpful data collection and discussion at 01B1-1 station, Canadian Light Source.

References

Budevska, B. O. (2002). *Handbook of Vibrational Spectroscopy*, Vol. 5, edited by J. M. Chalmers and P. R. Griffiths, pp. 3720–3732. New York: John Wiley and Sons.

Colthup, N. B., Daly, L. H. & Wiberley, S. E. (1990). *Introduction to Infrared and Raman Spectroscopy*, 3rd ed., p. 547. Boston, MA: Academic Press.

Cytospec (2004). *Software for Infrared Spectral Imaging.* Version 1.1.01. Cytospec, NY, USA.

Himmelsbach, D. S., Khalili, S. & Akin, D. E. (1998). *Cell Mol. Biol.* **44**, 99–108.

Jackson, M. & Mantsch, H. H. (2000). *Encyclopedia of Analytical Chemistry*, Vol. 1, edited by R. A. Meyers, pp. 131–156. Chichester: John Wiley and Sons.

Kemp, W. (1991). *Organic Spectroscopy*, 3rd ed. New York: W. H. Freeman.

Marinkovic, N. S. & Chance, M. R. (2006). *Encyclopedia of Molecular Cell Biology and Molecular Medicine*, Vol. 13, 2nd ed., edited by R. Meyers, pp. 671–708. New York: Wiley.

Marinkovic, N. S., Huang, R., Bromberg, P., Sullivan, M., Toomey, J., Miller, L. M., Sperber, E., Moshe, S., Jones, K. W., Chouparova, E., Lappi, S., Franzen, S. & Chance, M. R. (2002). *J. Synchrotron Rad.* **9**, 189–197.

Martin, M. C. (2002). *Fourier tranform infrared spectroscopy*, http://infrared.als.lbl.gov/.

Mathlouthi, M. & Koenig, J. L. (1986). *Adv. Carbohydr. Chem. Biochem.* **44**, 7–89.

Miller, L. M. (2000). *Synchrotron Rad. News*, **13**, 31–37.

Miller, L. M. (2002). *Infrared Microsperctroscopy and Imaging*, http://www.nsls.bnl.gov/newsroom/publications/otherpubs/imaging/workshopmillerhighres.pdf.

Miller, L. M. & Dumas, P. (2006). *Biochim. Biophys. Acta*, **1758**, 846–857.

Pietrzak, L. N. & Miller, S. S. (2005). *J. Agric. Food Chem.* **53**, 9304–9311.

Raab, T. K. & Martin, M. C. (2001). *Planta*, **213**, 881–887.

Sockalingum, G. D., Bouhedja, W., Pina, P., Allouch, P., Bloy, C. & Manfait, M. (1998). *Cell Mol. Biol.* **44**, 261–269.

Vogel, J. P., Raab, T. K., Schiff, C. & Somerville, S. C. (2002). *Plant Cell*, **14**, 2095–2106.

Wetzel, D. L. (2001). *Proceedings of the International Wheat Quality Conference II*, Manhattan, Kansas, USA, May 2001, pp. 1–20.

Wetzel, D. L., Eilert, A. J., Pietrzak, L. N., Miller, S. S. & Sweat, J. A. (1998). *Cell. Mol. Biol.* **44**, 145–167.

Wetzel, D. L. & LeVine, S. M. (2000). *Infrared and Raman Spectroscopy of Biological Materials*, edited by H. U. Gremlich and B. Yan, pp. 101–142. New York: Marcel Dekkar.

Wetzel, D. L., Srivarin, P. & Finney, J. R. (2003). *Vib. Spectrosc.* **31**, 109–114.

Yu, P. (2005). *Appl. Spectrosc.* **59**, 1372–1380.

Yu, P. (2006). *Spectroscopy*, **20**, 229–251.